Microstructure development in cryogenically rolled oxide dispersion strengthened copper

S. M. S. Aghamiri[*,1] , S. Ukai[1], N. Oono[1], , R. Kasada[2], H. Noto[3], Y. Hishinuma[3], T. Muroga[3]

[1]*Graduate School of Engineering, Hokkaido University, Sappor 060-8628, Japan*

[2] *Institute of Materials Research, Tohoku University, sendai 980-8577, Japan*

[3]*National Institute of Fusion Science, Gifu 509-5202, Japan*

Abstract

Recently, advanced oxide dispersion strengthened (ODS) copper alloys have been developed using mechanical alloying process as a fusion material. In this study, to develop a superior ODS copper alloy containing 0.5wt% Y_2O_3, the effect of cryogenic rolling on microstructure development and tensile properties was studied using high resolution EBSD, TEM and tensile tests. During cryogenic deformation of ODS copper, grain structure remains in submicron size scale as a combinatorial result of geometrically effects, nanotwin bundle deformation, interaction of dislocations with fine oxide particles and some diffusional processes including static recovery and recrystallization. Clear microstructural characterizations confirmed nucleation of fine new oriented recrystallized grains mainly on the HABs of 80%cryogenic rolled ODS copper. Quantitative analyses indicated grain boundary migration at room temperature following cryogenic deformation originated from high driving force induced by grain boundary bulging and high mobility induced by vacancies. The tensile properties of cryogenic deformed samples showed superior tensile strength than room temperature deformation leading to UTS: 624MPa, el_t: 5.5%, while saturation of strength between 60%-80% reduction, approved occurrence of softening by diffusional processes.

Keywords: ODS copper, Cryogenic rolling, Microstructure development, Recrystallization, Tensile properties

---

[*] Corresponding author. Hokkaido University, Sapporo 060-8628, Japan.

Email Address: sms.aghamiri@gmail.com

1. Introduction

Advanced oxide dispersion strengthened (ODS) copper alloys are attractive category of structural energy materials for high heat flux applications due to high mechanical properties and irradiation resistance [1,2]. It has been observed that distribution of nanoscale oxide particles in metallic matrix has a great influence on control of microstructure by pinning of dislocation/grain boundaries [3]. In fact, during deformation, a higher level of strain is accumulated in microstructure of ODS materials by formation of dislocation loops around nondeformable oxide particles known as geometrically necessary dislocations based on Orowan mechanism [4]. In other side, there is currently a great attention to development of nanocrystalline/ultrafine grained structural materials in order to achieve high strength and ductility. Up to now, the efforts by plastic deformation methods in copper such as heavy room temperature rolling or severe plastic deformation (SPD) processes could reach to a limited level of ultrafine grains of several hundred nanometers even at high strains. Such a minimum grain size was attributed to thermally activated processes, i.e. operation of dynamic recovery even at room temperature [5]. To suppress these processes and as a result reach a lower grain size in the range of nanocrystalline size, deformation at very low homologous temperature known as cryogenic deformation has been proposed [5-8].

In recent years, considerable studies have performed to understand the main mechanisms governing grain structure development especially in fcc alloys of aluminium and copper. One main mechanism studied during cryogenic rolling is geometrical effects of strain. It has been observed that a heavily elongated grain structure form in both aluminium [6] and copper [9] aligned in rolling direction without any significant grain fragmentation or subdivision. Furthermore, the grain structure includes a high fraction of

low angle grain boundary inside the individual grains. However, geometrical effects have been observed to saturate after a certain amount of strain (a true strain of 2.7 for copper) and the grain size does not refine anymore remaining in the range of submicron size. This behavior has been attributed to high thermally activated grain boundary migration which prevents formation of nanocrystalline grain structure in aluminium and copper [9]. Another active mechanism operating in medium stacking fault energy fcc materials like copper at cryogenic temperatures is mechanical twinning. The mechanical twins were reported to be in the bundle arrangement and typically in nanosized range. It has been confirmed that twinning has a great contribution in grain refinement during subsequent deformation by fragmentation of deformation twins forming nanoscale twin/matrix (T/M) lamella which has resulted in formation of nanosized grain at cryogenic temperatures [7,8]. Additionally, development of shear bands at high strain rate may induce fragmentation and rotation of the T/M lamellae, forming nanoscale elongated or equiaxed grains [7]. However, it is believed that cryogenic rolling of copper doses not result in nanocrystalline grain size due to limited twinning and shear banding [9].

A thorough literature survey shows that one unusual behavior of cryogenic deformed copper is recrystallization or in some case grain growth at room temperature [9-13]. It is hypothesized that the microstructural instabilities are attributed to a high density of vacancies in the cryodeformed material, giving rise to the exceptionally high grain-boundary mobility [14]. Although different studies have been paid to the mechanisms of recrystallization in pure copper in recent years, but still there is a low information on oxide dispersion strengthened copper alloys.

Development of crystallographic texture has been used as one effective approach to study the microstructural evolution during rolling deformation. It has been observed generally that fcc materials develop two different types of rolling texture especially depending on stacking fault energy (SFE) [15-16]: α-fiber in low SFE materials and β-fiber in medium to high SFE materials. The α-fiber is described by a combination of the brass orientation ($\{110\}\langle 2\bar{1}1\rangle$) and the Goss orientation ($\{110\}\langle 100\rangle$) while the β-fiber is obtained by the main orientations of copper ($\{112\}\langle 111\rangle$) and S ($\{123\}\langle 634\rangle$). It is widely accepted that β-fiber (copper type texture) is developed by homogenous deformation of $\{111\}\langle 110\rangle$ slip, but still the underlying mechanisms related to the formation of α-fiber (brass type texture) is under study. Deformation twinning has been noticed to have significant effect on development of the α-fiber texture via overshooting/latent hardening introduced by the closely spaced twin lamellae [17]. Recently, Gu et al. [18] discussed the deformation mechanism of brass-type texture in rolling of ultrafine-grained copper associated with the activation of partial $\{111\}\langle 11\bar{2}\rangle$ slip in addition to usual $\{111\}\langle 110\rangle$ slip and with a reduced quantity of geometrically necessary dislocations. Compared to pure copper, room temperature rolling of ultrafine grained ODS copper showed deformation mechanism of partial slip by $\frac{a}{6}\langle 211\rangle$ dislocations facilitated by the pinning of $\frac{a}{2}\langle 101\rangle$ perfect dislocations through fine oxide particles is responsible for formation of Brass texture [1].

Following to our previous study on microstructural evolution of ODS copper leading to a surprisingly single crystal like brass texture deformed grain during rolling at room temperature which resulted in a significant tensile properties [1], study of microstructural and mechanical evolution of ODS copper including nanoscale oxide

particles at cryogenic temperatures in view of both scientific and technological aspects on development of copper alloys with superior properties is an attractive subject. Furthermore, there is a weak understanding in literature on the role of fine nanoscale oxide precipitate during deformation in low temperatures. Therefore, the objective of this study is evaluation of microstructure development of ODS copper using electron back scatter diffraction (EBSD) approach with its advanced characterization techniques coupled with detailed microscopy observation and investigating the subsequent tensile properties after cryogenic deformation.

2. Experimental

In this study, an ODS copper material with a nominal composition of Cu-0.5wt% Y_2O_3 was prepared using mechanical alloying of primary powders and consolidation by spark plasma sintering. The details of fabrication can be found elsewhere [19]. Then the sintered ODS copper with the size of ~ 15 mm (diameter) × 10 mm (height) was cut in a thickness of 3 mm normal to the radial direction and subjected to subsequent cryogenic rolling and microstructural analysis.

Cryogenic rolling process was performed on the sintered ODS copper sample using liquid nitrogen at different thickness reductions of 20%, 40%, 60% and 80% and a low thickness reduction of 0.01 mm per pass using a two-rolling mill with the roll diameter of 160 mm. The evolution of microstructure and rolling texture during deformation was evaluated by stopping the cryogenic rolling process at each thickness reduction. In order to provide cryogenic deformation conditions, the specimen was soaked in liquid nitrogen prior to each rolling pass. Immediately after each pass, the sample was reinserted into

liquid nitrogen. However, to remove the cracks formed during rolling, sometimes the rolling was stopped, and the sample exposed to room temperature. After completion of the rolling process, specimen was stored in a freezer at ~ -10ºC.

The microstructure of specimens was observed by electron backscatter diffraction (EBSD) equipment attached to a field emission scanning electron microscope (JEOL JSM-6500F) operating at 15 kV. The observations were made on the rolling plane containing rolling direction (RD) and transverse direction (TD) in the mid-thickness section of the samples in 2 different magnifications with the step sizes of 40 and 80 nm. Sample preparation for EBSD was done by grinding with SiC paper up to 2000 grit and then polishing with 1 μm diamond paste and final polishing with Struers colloidal silica suspension. To attain EBSD data, TSL-OIM software was used for different analyses of inverse pole figure (IPF) maps, grain boundary map, grain orientation spread (GOS), orientation distribution functions (ODF) and grain size measurements. To improve the reliability of the EBSD data, small grains comprising three or fewer pixels were automatically removed from the maps using the grain-dilation option in the software. Furthermore, a lower limit boundary-misorientation cutoff of 2° was used and a 15° criterion was employed to differentiate low-angle boundaries (LABs) and high-angle boundaries (HABs). Grain size was quantified by the determination of the area of each grain and the calculation of its circle-equivalent diameter (grain reconstruction method). To evaluate the texture, ODF related to three different sections in $\varphi_2 = 0°, 45°, 65°$ were studied based on the typical orientations of fcc structures.

A JEOL JEM-2010 transmission electron microscopy was used with a voltage of 200 kV to study the microstructures of cryogenic rolled sample in high magnification.

The thin foil for TEM observation was prepared by focused ion beam (FIB) (JEOL JIB-4600F) and the thinning was accomplished up to the thickness of ~100 nm. For evaluation of oxide particle distribution, the average particle size and the number density of oxide particles was derived in thin foil based on TEM images using the convergent-beam technique [19].

In order to evaluate the evolution of mechanical properties, uniaxial tensile tests were performed parallel to the rolling direction at ambient temperature under a strain rate of $1.0 \times 10^{-3}\ s^{-1}$ using Shimadzu, SSL-1KN tensile machine. For each condition, two miniaturized size specimens were prepared with a gauge dimension of 5 mm in length, 1.2 mm in width and 0.5 mm in thickness using an electro-discharge processing machine.

3. Results and discussion

3.1. Microstructure ODS copper before Cryogenic rolling

The microstructure of ODS copper prior to cryogenic rolling prepared by mechanical milling and subsequent consolidation by spark plasma sintering at 900ºC/45min was characterized in previous work [1] to have equiaxed grains with mainly fine submicrometer grains with an average grain size of 0.23μm. The misorientation angle distribution of boundaries showed a high number fraction ~42% of low angle boundaries (<15º). The High angle boundaries had a peak around 60º indicating formation of annealing twins with a fraction of ~14% in the microstructure. Evaluation of crystallographic texture of grains demonstrated the main α-fiber with the intensity of 2.7 including Goss orientation ($\{011\}\langle 100\rangle$) to around Brass orientation ($\{011\}\langle 2\bar{1}1\rangle$)

together with weaker texture near to β-fiber (including copper $\{112\}\langle 111\rangle$ and S$\{123\}\langle 634\rangle$) and Y orientation ($\{111\}\langle 2\bar{1}1\rangle$).

3.2. Microstructural evolution after cryogenic rolling

3.2.1 Grain structure evolution

Low resolution orientation maps of rolling plane containing RD-TD for cryogenically rolled ODS copper sample after different thickness reductions of 20%, 40%, 60%, and 80% have been shown in Fig. 1. It is evident that the evolution of fine submicron grains based on the orientation and shape is happening during cryogenic rolling. To follow the grain size evolution, the mean grain size has given as equivalent diameter by assumption of grains as circular shape for different reductions in Fig. 2. As observed in Fig. 1 (a), after 20% reduction, the grains are mainly in the range of submicron sized with an average size of 0.26 μm and have equiaxed shape. Increasing reduction to 40%, change partial orientation of grains as indicated by color map and some parts of the grains tend to change to a different elongated shape (Fig. 1(b)). In 60% reduction (Fig. 1(c)), the low-aspect ratio grains have changed widely to elongated pancaked shape grains in the rolling direction by extensive grain compression without any appreciable change in grain size between 20 to 60% reductions (Fig. 2). This observation specifies the main mechanism is still geometrical effect by compression and extension of grains in the rolling direction. Continuing cryorolling to highest 80% reduction results in considerable evolution in shape and grain size so that the partial grains transform to equiaxed shape with increment of average grain size to 0.43 μm. It should be noted that the increasing of the standard deviation indicates developing a wider range

of grain size for 80% reduction. This determines other mechanisms than geometrical effects are governing the grain structure evolution in heavy cryorolling.

To study the grain structure evolution in more details, grain boundary maps cryogenically rolled ODS copper sample after different thickness reductions of 20%, 40%, 60%, and 80% have been provided with high magnification of 1 micron scale in Fig. 3. In these images, the low angle grain boundaries of 2-5° and 5-15° have been shown in red and green colors, respectively and high angle boudaries of >15° are in black color. To compare quantitatively, the evolution of LABs (2-15°) and HABs (>15°) during increasing cryogenic rolling reductions has demonstrated in Fig. 4 based on misorientation angle distribution diagrams. As observed in Fig. 4(a), the main grain structure at the low rolling reduction of 20%Re is as HABs and in some area the grains are devided by low angle boudaries. It should be noted that this increas of HABs to a number fraction of ~63% in compared to initial condition resulted in little decrese of grain size as shown in Fig. 2. Then, increasing the rolling reductions results in increasing the number fraction of LABs to number fractions of 57% and 43% in 40%Re and 60%Re, respectively. This promotion of LABs is interpreted by development of deformation-induced boundaries during cryogenic rolling [20] and is in contrast to little change of LABs during room temperature rolling of ODS copper [1]. The black HABs can be seen as partially elongated in the direction of rolling and their fraction decrease with promoting of the fraction of substructures inside the grains. In other side, the red LABs are short and in some case have curved shapes distributed inside the grains or near HABs while the green LABs are continuous and may be the result of grain-subdivision process [9]. After

80%Re, the grains shape change considerably along with decresing the number fraction of HABs as expected by promotion of grain size.

TEM observation has performed for heavily 80% cryorolled ODS copper sample some days after accomplishing cryorolling. The low magnification Bright-field TEM image in Fig. 5 (a) show the fine submicron grains alligned in the rolling direction have been developed including some substructutures containing deformation induced boundaries (DIBs). The inset selected area diffraction pattern suggests several grains including finer subgrains are located together with different orientations. The higher magnification image of grain structure was provided in Fig. 5(b) to present the grain interiors in higher resolution. As clearly observed, except some hevily deformed area with a sharp contrast variations, a high area of the microstructure show a homogenous TEM contrast and a low dislocation density suggesting of dislocation annihilation and annealing of deformed microstructure has happened after cryogenic deformation probably during room temperature storage. The similar characteristic has been reported by Konkova et al. [9] after cryogenic deformation of pure copper, however in the case of ODS copper alloy, the governing evolution mechanism has occurred in ultrafine/nanometer scale by controlling the microstructure via nanoscale oxide particles. Recently, the annealing of cold rolled ODS copper has been confirmed as a result of recovery process during long time storage at room temperature [20]. In other side, observation of severly deformed area in high resolution presents two important microstructural features; as shown in Fig. 5(c), nanotwin bundles have formed with a fine lamellae thickness of less than 2 nm and a length up to 50 nm in different deformed area. Analysis of the twin boundaries showed that there is no ideal twin/matrix relationship as

explained in the literature as strain-induced crystallographic rotation during deformation. Such a fine deformation twins has been reported for cryogenic deformation of copper [7,9,15]. In addition, interaction of nanosized oxide particles with dislocations can be seen in Fig. 5(d). In the figure, fine semicoherent oxide particles with a size of <10 nm indicated by moire fringe contrast [21] distributed in the deformed matrix are interacting with different black lines of dislocations. It demonstrates pinning of dislocation by fine oxiede particles established by Scattergood and Bacon [22] based on the Orowan mechanism as discussed during deformation of ODS copper in details in previous work [1].

3.2.2. Texture evolution

The evaluation of crystallographic texture during rolling of fcc metals especially copper alloys has performed widely in literature and is an effective instrument to study the microstructural development [1,4,9,10,15]. In Fig. 6(a-d), the evolution of crystallographic texture during cryogenic rolling of ODS copper at different thickness reductions of 20%, 40%, 60% and 80% has been shown based on ODF at φ_2=0°, 45°,65° derived from large EBSD scans containing ~2500-7000 grains. The fraction of each texture components was depicted in Fig. 7 as a function of cryogenic rolling reduction. Furthermore, distribution of individual texture components was specified in the cryogenic rolled microstructures as assigned colors to determine the arrangement and morphology of different crystal orientations.

In 20%Re, a α-fiber texture including Goss orientation (011) [100] with intensity of 1.9 times and Brass orientation (011) [2-11] with intensity of 1.5 times, in addition to a higher intensity (3.2 times) orientation of (112) [1-10] have been developed (Fig. 6(a)).

All the main texture components have been weakened in compared to initial material and instead some transient texture has been evolved (Fig. 7). The ideal texture orientations have been distributed as fine submicron sized equiaxed grains (Fig. 8).

In 40%Re, the maximum texture intensity becomes stronger (~10.7 times) and some major change happened: the α-fiber texture splitted to stronger Goss orientation ((110) [100] *10) and Brass texture was weakened and moved toward P orientation ((011) [2-11]). In addition, some specific unstable orientations can be seen to develop in $\varphi_2 = 45°$ and 65°: (111) [-1-12] with intensity of 4, (212) [1-41] with intensity of 8.2, (221) [-2-23] with intensity of 4. Interestingly, the fraction of Goss and Copper orientations has increased sharply as typically large and elongated grains in 40% rolled microstructure (Fig. 7 and 8).

After higher reduction of 60%Re, the approximate fcc rolled texture is developing with a maximum intensity of 5.4 times as stronger α-fiber including Goss and Brass orientations and weaker β-fiber texture passing through of copper orientation ((112) [111]) and near S orientation ((212) [-1-22]). In this step, the Brass and S textures tend to increase as thin elongated grains in the rolling direction compared to decreasing trend of Goss and S orientations (Fig. 7 and 8).

In final cryogenic rolling of 80% Re, the texture becomes fully developed in ideal rolled texture based on Table 1 and maximum intensity increases to 9.5 times with development of both stronger α-fiber (~7.5 times) and weaker β-fiber texture (~3.6 times). The Brass and S components have the highest fraction (each about 20%) and can be observed as large and random irregular distribution in the microstructure.

The present texture development in Fig.7 shows peaks of Copper and Goss orientations at 40%reduction in contrast to peaks of Brass and S orientations at

80%reduction. This transient Copper-type texture may be interpreted based on perfect slip mechanism vs brass type texture by twinning mechanism in higher reductions [17]. Furthermore, the texture development of 80% cryogenic rolled ODS copper is in sharp contrast to single Brass texture of 80% room temperature rolled ODS copper by deformation mechanism of partial slip [1]. As deformation mechanism is closely dependent on the deformation temperature, the change of texture at cryogenic temperatures is expected to happen due to extensive fine deformation twinning mechanism as explained in previous section or probable suppression of cross-slip hypothesized for cryogenic deformation of copper [9].

Actually, the final texture of 80% cryogenic rolled ODS copper is comparable to texture development of pure copper after 93% cryogenic rolling in Ref. [9]. This is explained by effect of nanoscale oxide particle dispersion in the microstructure which expose higher amount of internal strain by formation of geometrically necessary dislocations during deformation based on Ashby model [4]. Some similarity with the texture of recrystallized ODS copper after high temperature annealing [1] reminds that another microstructural characteristic for changing the texture is attributed to the recrystallization phenomena which will be discussed in detail in the next section.

3.2.3. Recrystallization

In order to characterize the effect of thermally activated processes such as recrystallization on grain structure evolution, the microstructure of 80% cryogenic rolled ODS copper was studied by advanced techniques of high-resolution EBSD in Fig. 9. It should be noted the sample was observed about 10 days storage in low/room temperature for preparation and characterization after cryogenic rolling. Fig. 9(a) demonstrate that

some fine nano/submicron sized grains are nucleating with new orientations as indicated by different colors between the deformed grains. The corresponding grain boundary map (Fig. 9(b)) shows that the new grains have bordered by HABs in blue color and typically are free of substructure in contrast to the deformed matrix including a considerable LABs<15° in red/green colors. These fine grains are mainly nucleated on HABs of pre-deformed grains as specified by circles and in some cases are nucleated on LABs as shown by squares. A low value of grain orientation spread typically less than 1° is seen in the GOS map (Fig. 9 (c)) as bright contrast grains in contrast to deformed grains as dark contrast ones. To measure the grain orientation spread, an average misorientation between each pixel of a grain and the average orientation of the grain is calculated. The recrystallized grains are usually defined as those having an orientation-spread below ~2° [10-12]. So, the characterizations clearly confirm that fine new orientated recrystallized grains surrounded by HABs and free of subgrains are nucleating inside the cryorolled microstructure.

The observation of the 80% cryogenic rolled ODS copper sample by transmission electron microscopy in Fig. 10 reveals more aspects of evolution of microstructure after about 10 days storage at low/room temperature. Fig. 10 (a) shows the band like severely deformed grains of 80% cryogenic rolled with alignment of a few grains in the rolling with different orientations based on the inset diffraction pattern in upper part of figure. In the center part, it appears some fine grains of ~30-50 nm indicated by red arrows with a bright direction contrast which regarded as recrystallized grains in the grain/subgrain boundary of deformed grains. The diffraction pattern (DP) from the circle line shown in the lower part of figure indicates that a new crystalline orientation nucleated with a zone

axis of [211] between the deformed grains. Fig. 10 (b) depicts another recrystallized grain of low density of defects with a size of ~200 nm including fine dispersion of oxide particles as indicated by arrows. Evaluation of grain boundaries suggest that one side of the grain have a flat and curved shape boundary which is the probable starting point of recrystallized nuclei on the high angle boundary while the other side of grains shows different grain boundary bulges with a radius of ~20 nm as the front of recrystallized grain boundary. Fig. 10 (c) demonstrates some broken boundary between neighboring grains (as indicated in oval shape) with different stored energy which are hypothesized as the potential nuclei for development of recrystallized grains during annealing. In Fig. 10 (d), one another grain of ~100 nm×70 nm can be seen surrounded by heavily deformed grains which includes a low dislocation/defect density and divided into some subgrains. The DPs from different areas inside the grain as shown in inset figures show that there is low misorientation between different area with straight boundaries which are probably polygonised into finer subgrains with arrangement of dislocations inside the grain and reminds the process of static recovery as a dominant microstructural factor. The role of static recovery has also been discussed recently in the process of recrystallization of cold rolled oxide dispersion strengthened copper/pure copper during room temperature annealing [10,11].

Although there are some reports discussing on the possibility of recrystallization in room temperature in copper alloys from some decades ago, however, the detailed and quantitative discussion on the process of recrystallization at such a low temperature (~0.22 T_m) is still lacking. In order to evaluate the progress of recrystallization, it needs to study the velocity of grain boundary migration (V) as the following equation [23]:

$$V = M \times \Delta G_t \quad (3\text{-}1)$$

where, M is the grain boundary mobility and ΔG_t is the total driving force of grain boundary migration. The grain boundary mobility is considered as the following relation [23]:

$$M = \delta\, \vartheta \exp(-Q/RT)/RT \quad (3\text{-}2)$$

where δ and ϑ are the distance and atomic jump frequency across the boundary ($0.0635nm$ and $10^{13}s^{-1}\ for\ d_{\{110\}Cu}$), respectively, R is the universal gas constant (8.314 J/(mol. K)), and Q is activation energy for the atomic diffusion across the boundary taken as 17.8 Kcal/mol for high angle grain boundary according to Ref. [14]. Therefore, a grain boundary mobility of $1.92 \times 10^{-13}\, m^4/MJ.s$ could be obtained at room temperature (~300 K) which regarded as a high level to induce recrystallization. It is believed that high grain boundary mobility is associated with a high density of vacancies in the cryodeformed material, giving rise to the exceptionally high grain-boundary mobility [11-14]. In other side, the total driving force for grain boundary migration is calculated based on the following terms:

$$\Delta G_t = \Delta G_{st} + \Delta G_{gb} - \Delta G_{pin} \quad (3\text{-}3)$$

where ΔG_{st} is stored energy of dislocations, ΔG_{gb} is the grain boundary energy and ΔG_{pin} is the pinning force of oxide particles. The stored energy of dislocation is calculated by following equation [4]:

$$\Delta G_{st} = Gb^2\rho \quad (3\text{-}4)$$

where G denotes the shear modulus (45.5 GPa), b is the Burgers vector of the dislocations (0.255 nm) and ρ is dislocation density taken as value of 10^{15} m^{-2}, thus results in a stored energy of 2.96 MJ/m^3. Another term of grain boundary energy is evaluated based on the curvature of grain boundaries as following equation [4,23]:

$$\Delta G_{gb}=2\gamma\left(\frac{1}{r}-\frac{1}{R}\right) \quad (3\text{-}5)$$

where γ is the surface energy (~0.8J/m^2 [24]), r is the radius of the bulged boundaries (~typically 20 nm as experimental data in Fig. 10) and R is the average radius of grains (~ 220 nm in Fig. 2). Therefore, a high grain boundary energy of 72.56 MJ/m^3 is provided in the bulged boundaries. In compared to driving force induced by both dislocation density and grain boundary bulging, the fine oxide particles behave as opposing force against the grain boundary migration according to following relation by Nishizawa et al. [25]:

$$\Delta G_{pin}=\frac{3\sigma f^{2/3}}{4r} \quad (3\text{-}6)$$

where σ is the interface energy (~1 J/m^2), f and r are the volume fraction (~0.0075) and radius of oxide particles (~5 nm) according to previous study [19]. The obtained pinning energy is calculated to be ~5.7 MJ/m^3. The sum of the three discussed terms leads to a high value of total driving force of grain boundary migration (ΔG_t) around 70 MJ/m^3, which means a high driving force of grain boundary migration is resulted mainly from the energy induced by grain boundary bulging. Therefor, considering the amounts of grain boundary mobility and total driving force of grain boundary migration, a high velocity of

$1.34 \times 10^{-11} m/s$ is resulted based on equation (3-1) which is enough for development of submicron recrystallized grains just after several hours annealing at room temperature.

3.2.4. Tensile properties

The engineering tensile stress-strain curves of cryogenic rolled and room temperature rolled ODS copper at different thickness reductions of 20%, 40%, 60%, and 80% have been demonstrated in Fig. 11(a) and (b), respectively. The evolution of tensile properties including yield strength (YS), ultimate tensile strength (UTS), uniform elongation (el_u) and total elongation (el_t) have been evaluated in Fig. 12. As observed in the Fig. 12, in compared to room rolling, both YS and UTS have improved after cryorolling at all reductions with a highest strength of 624 and 550 MPa at 80%Re, respectively. This suggests occurance of dynamic recovery during/after deformation at room temperature rolling and stimulation of mechanical twinning at cryogenic deformation as the microstructural evolution after 80% cryogenic deformed ODS copper discussed in Sec. 3.2.1. However, although the level UTS and YS are increasing by enhacing of cryogenic deformation strain, saturation of both YS and UTS happens after 60% reduction in contrast to increment of strength during room rolling. This unusal behavior of cryogenic rolled ODS copper is a clear evidence of occurring softening during storing at room temperature associated with diffusional processes such as recovery and static recrystallization which are dominating at higher level of cryogenic deformation. These microstructural phenomena were previously discussed also for the pure copper by Konkava et al. [11-13]. In other side, the evolution of ductility shows sharp drop after 20% reduction for cryogenic rolling compared to annealed condition. The level of ductility (el_t

or el_u) is slightly lower in cryogenic deformation than room temperature at all reductions except total elongation (el_t) at 80% reduction attributed to unique microstructural evolution of single crystalline-like grain during rolling of ODS copper at room temperature as discussed in previous work [1]. In higher reductions, the changes of ductility become in slow rate leading to a final el_t of 5.5% and el_u of 2.3% at 80% reduction cryogenic deformation.

Conclusions

In this work, the microstructural characterization of ODS copper during cryogenic deformation was performed using EBSD and TEM observations and the mechanisms of grain structure development were accompanied by quantitative analyses and tensile properties. The main conclusions are as follows:

1. Grain structure evolution during cryogenic deformation of ODS copper is the result of geometrically effects, nanotwin bundle deformation and some diffusional processes including static recovery and recrystallization. The average grain size remains in the submicron size range with an increment after 80% reduction and change in the shape of grains associated with lowering the fraction of HABs.

2. The texture during cryogenic deformation of ODS copper change from some transient texture components at low reduction to ideal texture of α and β-fibers including higher intensity of Brass and S orientations at 80% reduction. This texture evolution is consistent with cryogenic deformation of pure copper and interpreted in terms of twinning deformation, suppression of cross-slip and limited recrystallization.

3. Static recrystallization of cryogenic rolled ODS copper was detected by

EBSD analysis and confirmed by quantitative analysis of grain boundary migration resulted from a high driving force induced by grain boundary bulging and high mobility induced by vacancies.

4. Cryogenic rolled ODS copper at different thickness reductions showed higher tensile strength as high as 624 MPa and a ductility of 5.5% at 80% reduction in compared to room temperature deformation and saturation of strength occurred by increasing of cryogenic deformation strain due to softening associated with diffusional processes of recovery and static recrystallization.

Acknowledgement

The authors gratefully acknowledge the JX Metal Co. for heat treatment of mechanically alloyed ODS copper powder in hydrogen atmosphere. The laboratory of Nano-Mirco Materials Analysis (NMA) is appreciated for using the analysis facilities. This work was supported by Grant-in-Aid for Scientific Research(A), 16H02443, Japan Society for the Promotion of Science (JSPS).

References

1. S. M. S. Aghamiri, N. Oono, S. Ukai, R. Kasada, H. Noto, Y. Hishinuma, T. Muroga, Brass-texture induced grain structure evolution in room temperature rolled ODS copper, Mater Sci. Eng. A 749 (2019) 118–128.
2. M. Li, S. J. Zinkle, Physical and Mechanical Properties of Copper and Copper Alloys, in: R.M.J. Konings (Eds.), Comprehensive Nuclear Materials, Vol. 4, Elsevier Ltd., 2012, 667-690.
3. D. A. Porter, K. E. Easterling and M. Y. Sherif, Phase transformations in metals and alloys, Third Edition, CRC press, 2009.
4. F. J. Humphreys, M. Hatherly, Recrystallization and related annealing phenomena, Second Edition, Elsevier, 2004.
5. Y. Wang, M. Chen, F. Zhou and En Ma, High tensile ductility in a nanostructured metal, Nat. 419 (2002) 912-915.
6. Y. Huang, P. B. Prangnell, The effect of cryogenic temperature and change in deformation mode on the limiting grain size in a severely deformed dilute aluminium alloy, Acta Mater. 56 (2008) 1619-1632.
7. Y. S. Li, N. R. Tao, K. Lu, Microstructural evolution and nanostructure formation in copper during dynamic plastic deformation at cryogenic temperatures, Acta Mater. 56 (2008) 230–241.
8. Y. Zhang, N. R. Tao, K. Lu, Mechanical properties and rolling behaviors of nano-grained copper with embedded nano-twin bundles, Acta Mater. 56 (2008) 2429–2440.
9. T. Konkova, S. Mironov, A. Korznikov, S.L. Semiatin, Microstructural response of pure copper to cryogenic rolling, Acta Mater. 58 (2010) 5262–5273.
10. S. M. S. Aghamiri, N. Oono, S. Ukai, R. Kasada, H. Noto, Y. Hishinuma, T. Muroga, Recrystallization of cold rolled oxide dispersion strengthened copper during room temperature annealing, J. Alloys Compd. 798 (2019) 187-193.
11.T. Konkova, S. Mironov, A. Korznikov, S. L. Semiatin, On the room-temperature annealing of cryogenically rolled copper, Mater. Sci. Eng. A 528 (2011) 7432–7443.
12.T. Konkova, S. Mironov, A. Korznikov, M.M. Myshlyaev, S.L. Semiatin, Annealing behavior of cryogenically-rolled copper, Mater Sci. Eng. A 585 (2013) 178–189.
13.T. Konkova, S. Mironov, A. Korznikov and S.L. Semiatin, Microstructure instability in cryogenically deformed copper, Scripta Mater. 63 (2010) 921–924.
14.H. D. Mengelberg, M. Meixner and K. Locke, the kinetics of the recrystallization of copper deformed at low temperatures, Acta Metall., 13 (1965), 835-844.
15.G. Anand, K. Barai, R. Madhavan, P.P. Chattopadhyay, Evolution of annealing texture in cryo-rolled copper, Mater Sci. Eng. A 638 (2015) 114–120.
16.Hirsch J, Lucke, Mechanism of deformation and development of rolling textures in polycrystalline f.c.c. metals—I. Description of rolling texture development in homogeneous CuZn alloys, Acta Metall. 36 (1998) 2863.
17.T. Leffers, R. K. Ray, The brass-type texture and its deviation from the copper-type texture, Prog. Mater. Sci. 54 (2009) 351–396.
18.C.F. Gu, L.S. Toth, Y.D. Zhang and M. Hoffman, Unexpected brass-type texture in rolling of ultrafine-grained copper, Scripta Mater. 92 (2014) 51–54.
19.S.M.S. Aghamiri, N. Oono, S. Ukai, R. Kasada, H. Noto, Y. Hishinuma, T. Muroga, Microstructure and mechanical properties of mechanically alloyed ODS copper alloy for fusion material application, Nucl. Mater. Energy 15 (2018) 17–22.

20.S.M.S. Aghamiri, S. Ukai, N. Oono, R. Kasada, H. Noto, Y. Hishinuma, T. Muroga, Recrystallization of cold rolled oxide dispersion strengthened copper during room temperature annealing, J. Alloys Compd.798 (2019) 187-193.
21.P. Dou, A. Kimura a, T. Okuda, M. Inoue, S. Ukai, S. Ohnuki, T. Fujisawa, F. Abe, Polymorphic and coherency transition of Y–Al complex oxide particles with extrusion temperature in an Al-alloyed high-Cr oxide dispersion strengthened ferritic steel, Acta Mater. 59 (2011) 992–1002.
22.R. O. Scattergood and D. J. Bacon, The Orowan mechanism in anisotropic crystals, Phil. Mag. A 31 (1975) 179-198.
23. S. Ukai, K. Taya, K. Nakamura, S. M.S. Aghamiri, N. Oono, S. Hayashi, T. Okuda Directional recrystallization by zone annealing in a Ni-based ODS superalloy, J. Alloys Compd. 744 (2018) 204-210.
24. E. A.Holm, D. L.Olmsted, S. M. Foiles, Comparing grain boundary energies in face-centered cubic metals: Al, Au, Cu and Ni, Scripta Mater. 63 (2010) 905–908.
25.T. Nishizawa, I . Ohnuma, K. Ishida, Examination of the zener relationship between grain size and particle dispersion, Mater. Trans. JIM 38 (1997) 950.

List of Figures

List of Tables

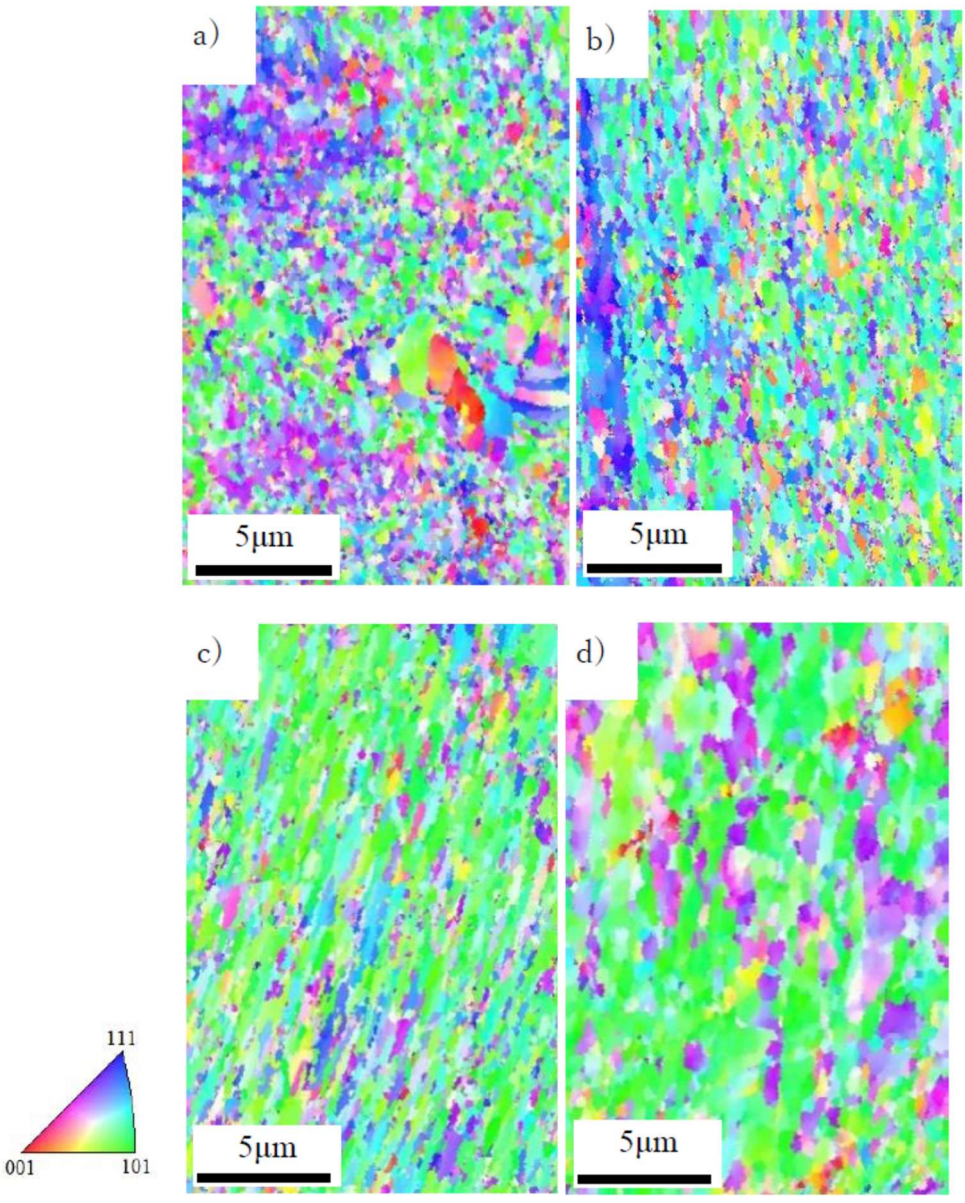

Fig.1

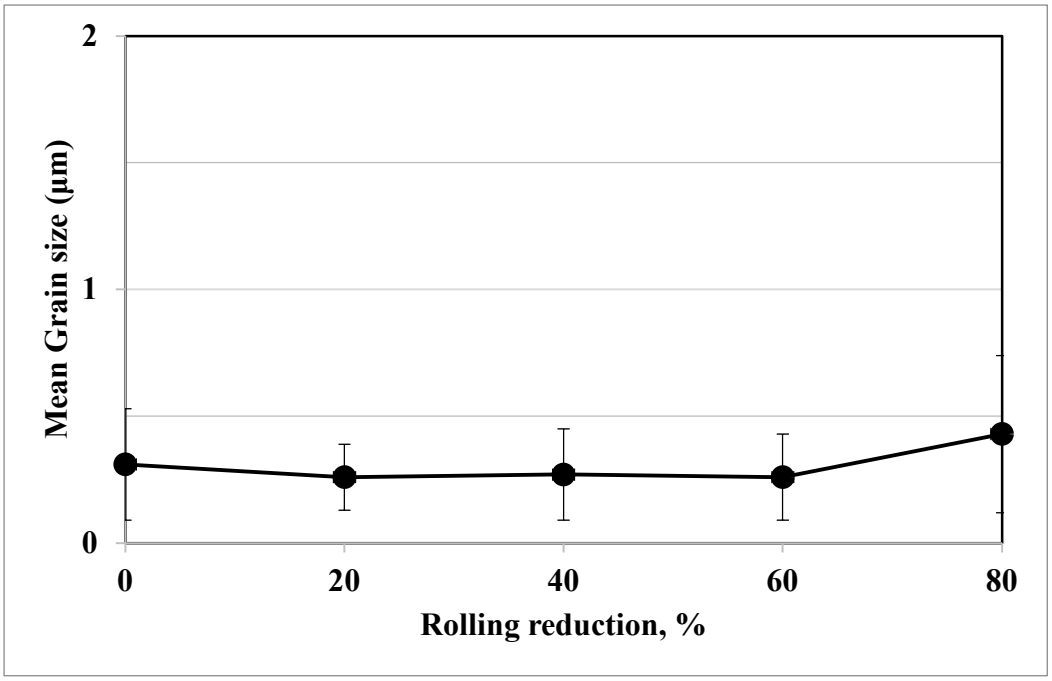
2
1
0
Mean Grain size (μm)
0
20
40
60
80
Rolling reduction, %

Fig. 2.

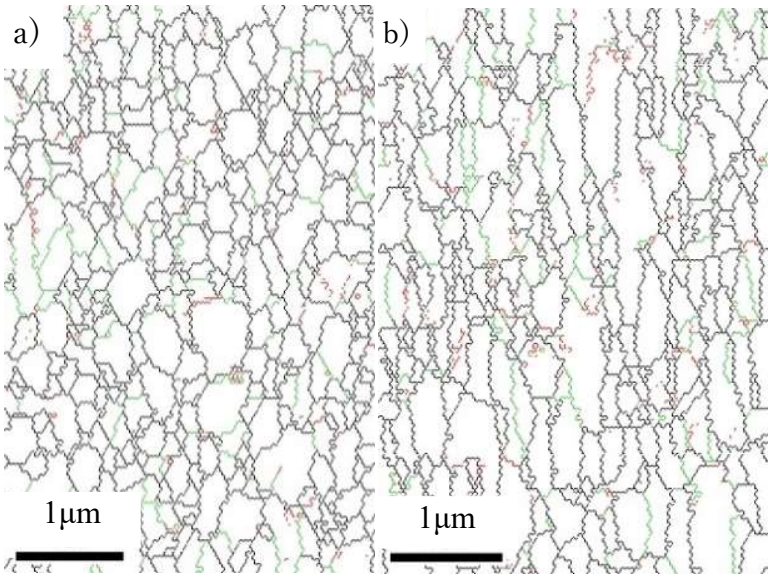
a)
b)
1μm
1μm

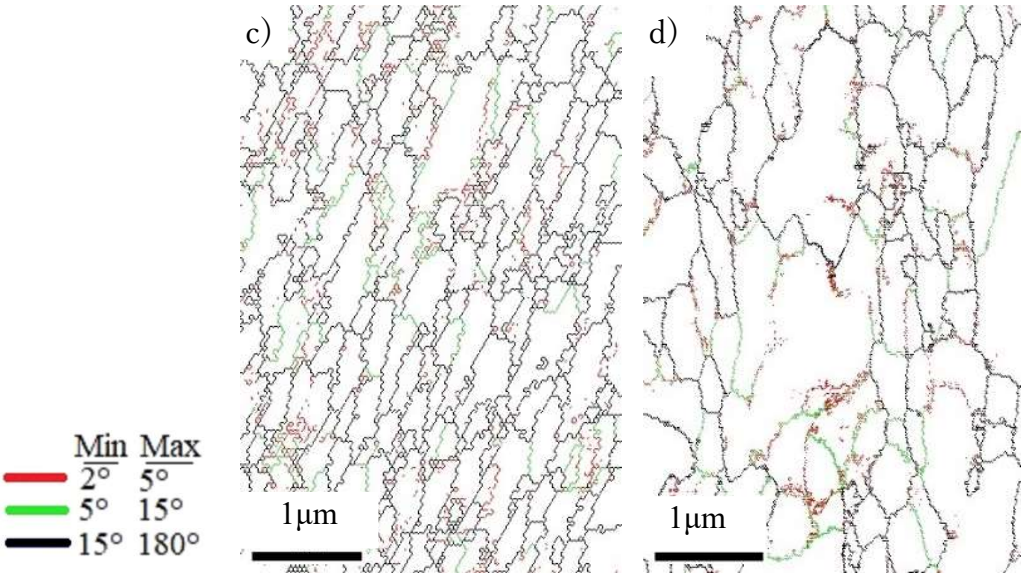
c)
d)
Min Max
2° 5°
5° 15°
15° 180°
1μm
1μm

Fig. 3.

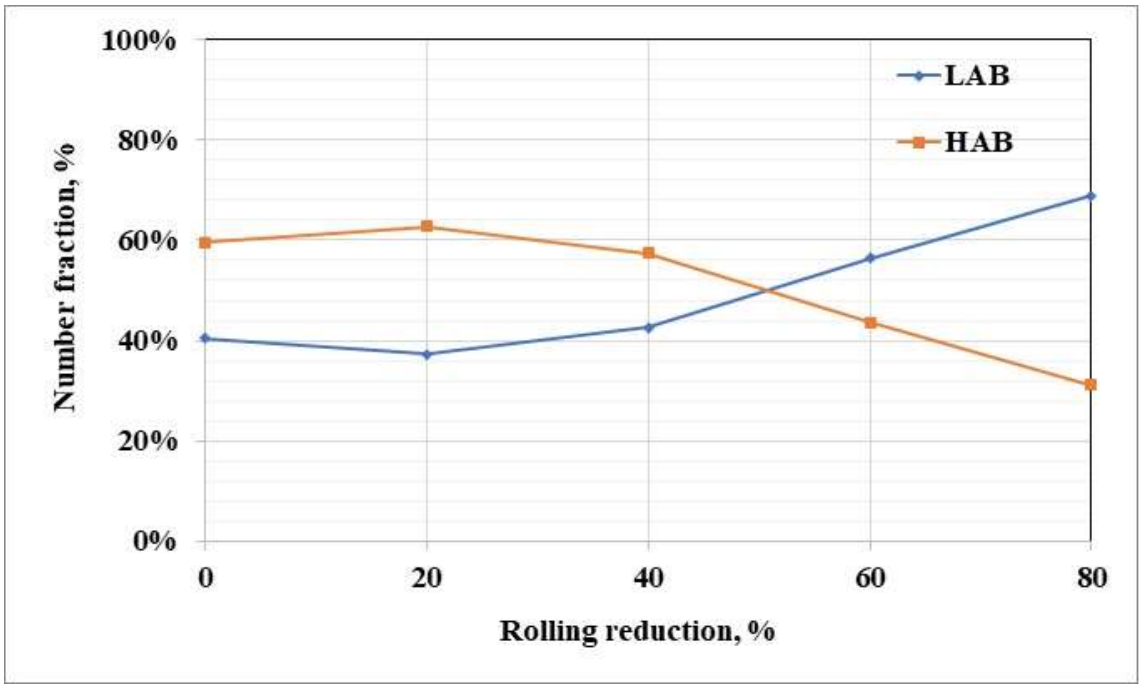
100%
80%
60%
40%
20%
0%
Number fraction, %
0
20
40
60
80
Rolling reduction, %
LAB
HAB

Fig. 4.

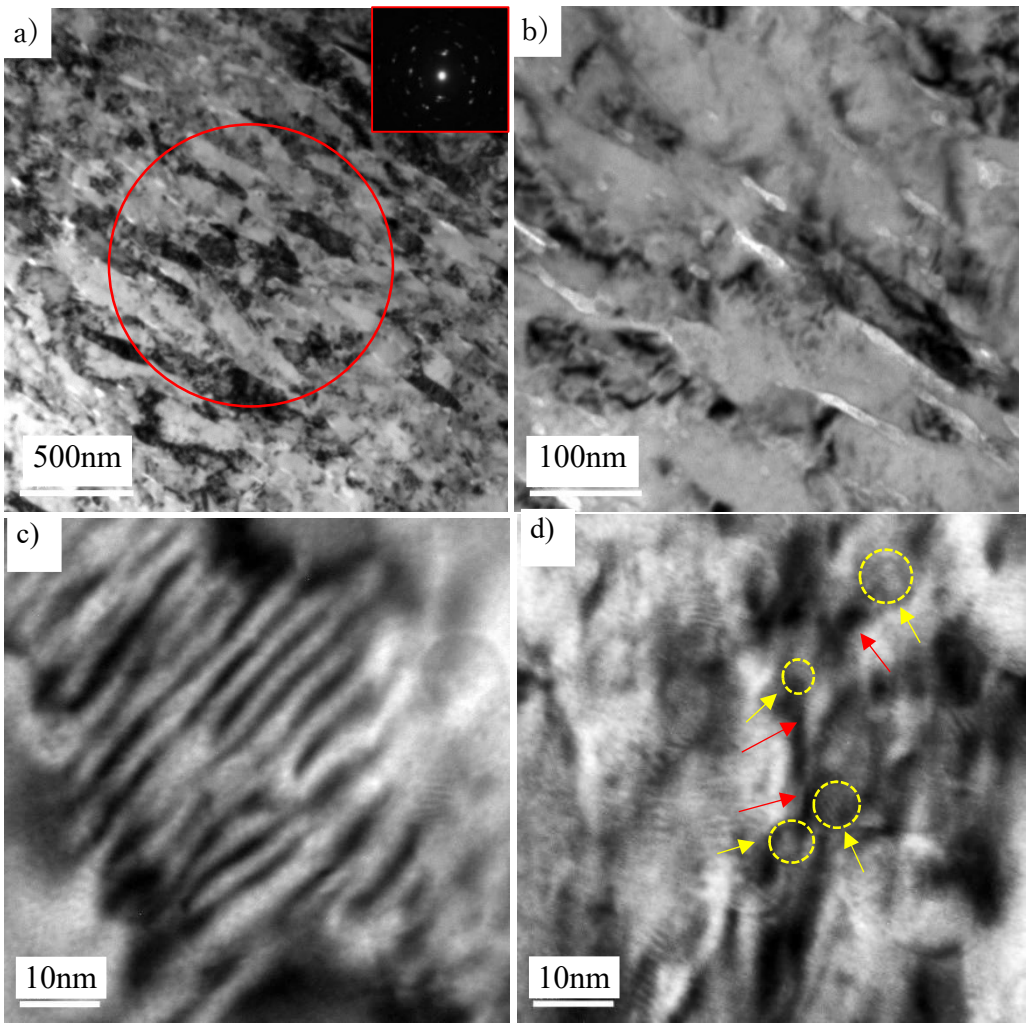

Fig. 5.

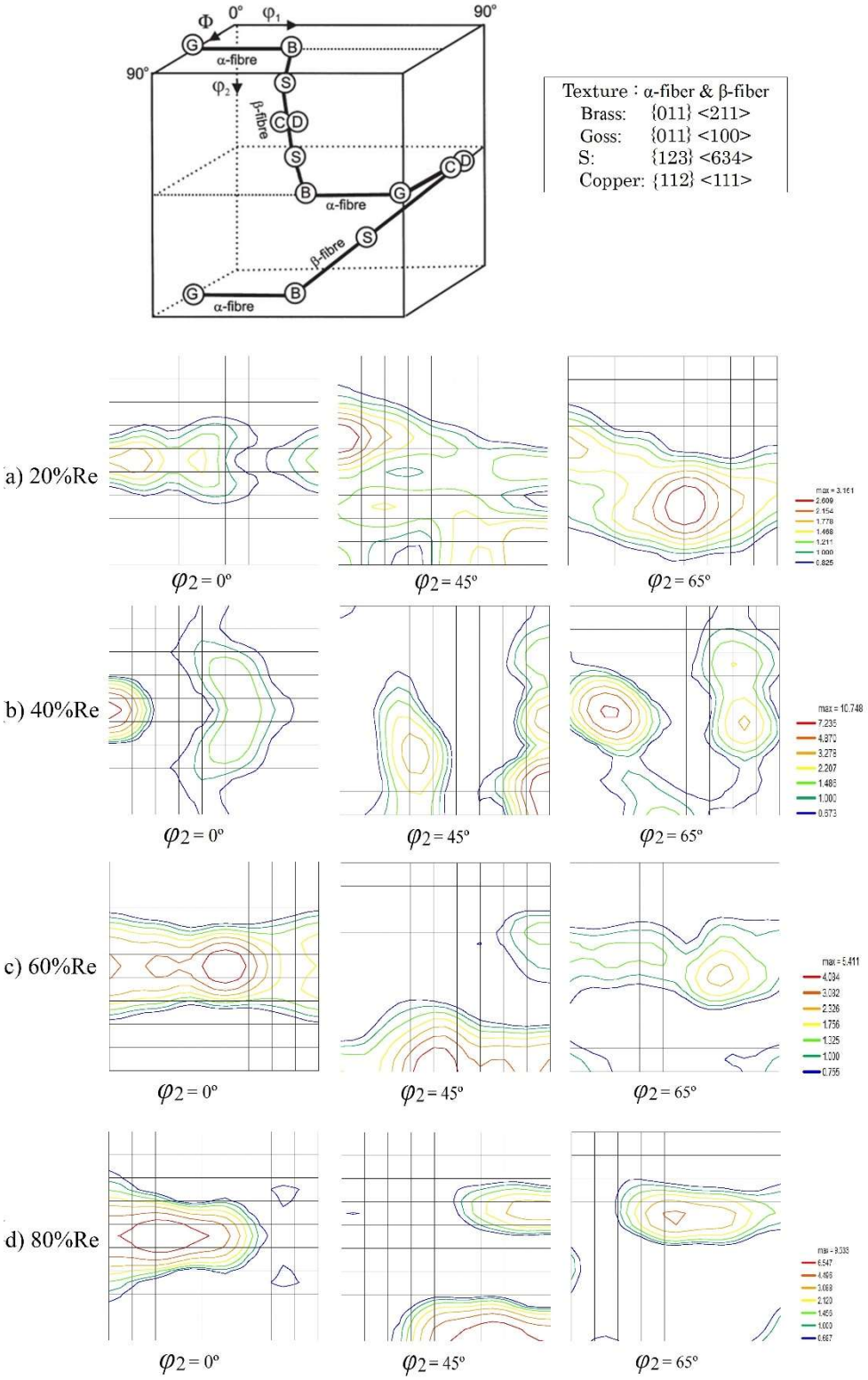
Φ
0°
φ1
90°
90°
φ2
α-fibre
β-fibre
α-fibre
β-fibre
α-fibre
G
B
S
C
D
Texture : α-fiber & β-fiber
Brass: {011} <211>
Goss: {011} <100>
S: {123} <634>
Copper: {112} <111>
a) 20%Re
b) 40%Re
c) 60%Re
d) 80%Re
φ2 = 0°
φ2 = 45°
φ2 = 65°

Fig. 6

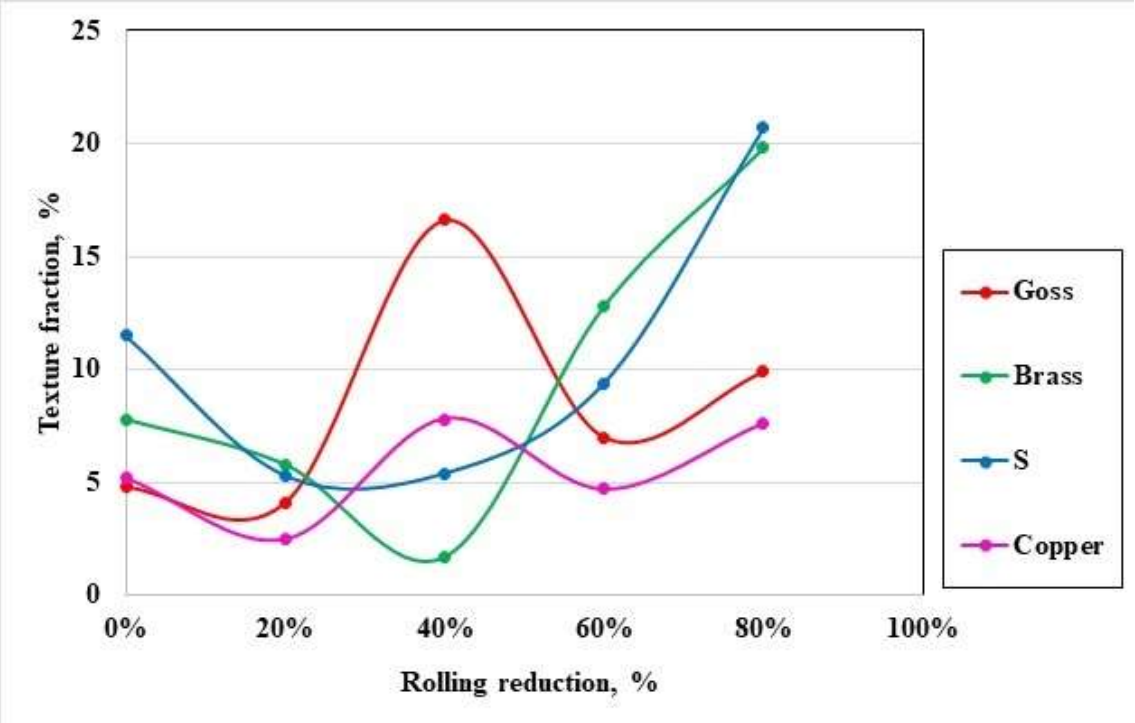
25
20
15
10
5
0
Texture fraction, %
0%
20%
40%
60%
80%
100%
Rolling reduction, %
Goss
Brass
S
Copper

Fig. 7

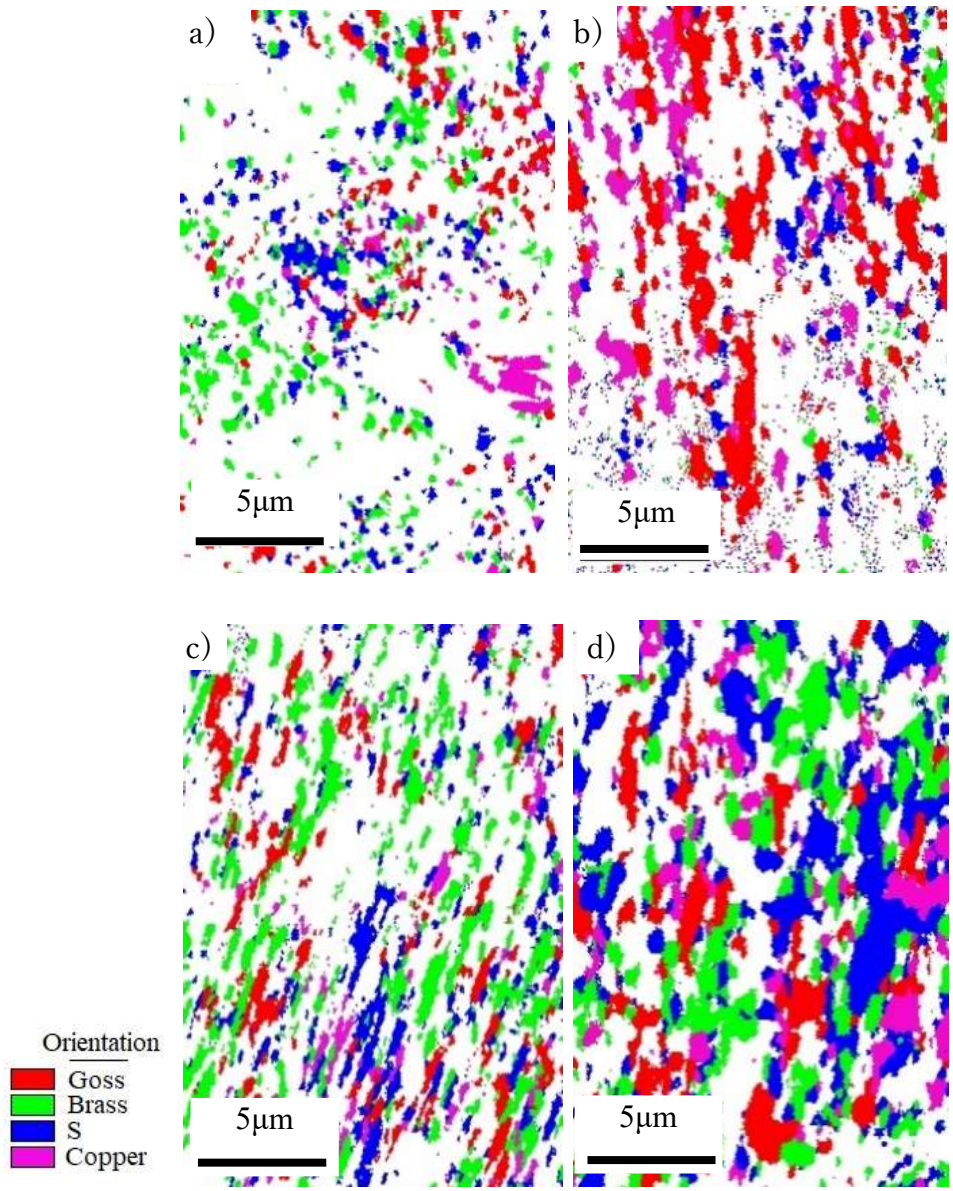

Fig.8.

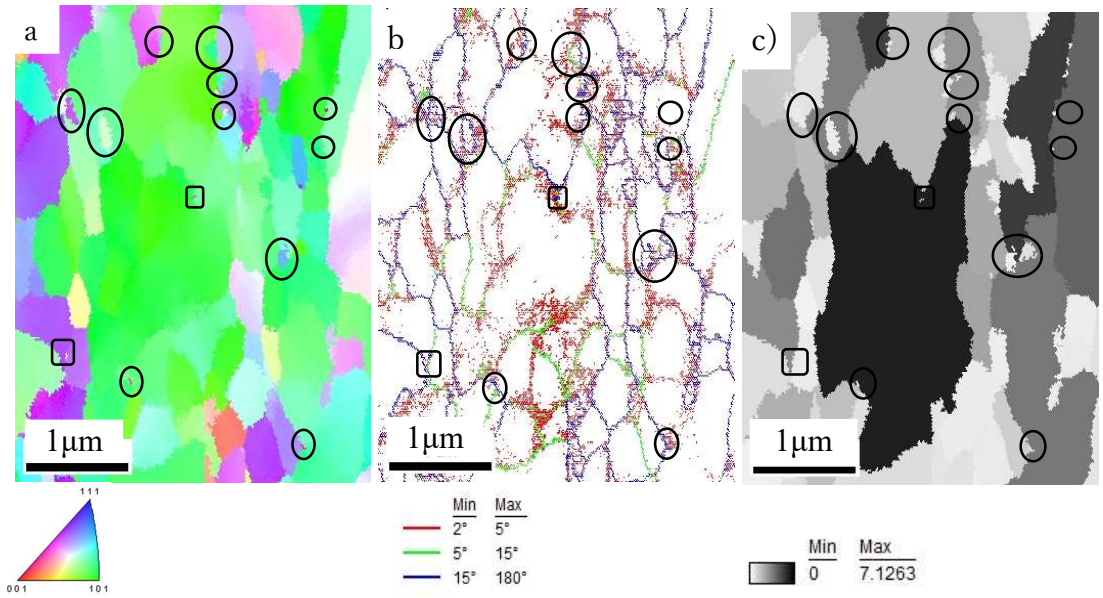

Fig. 9.

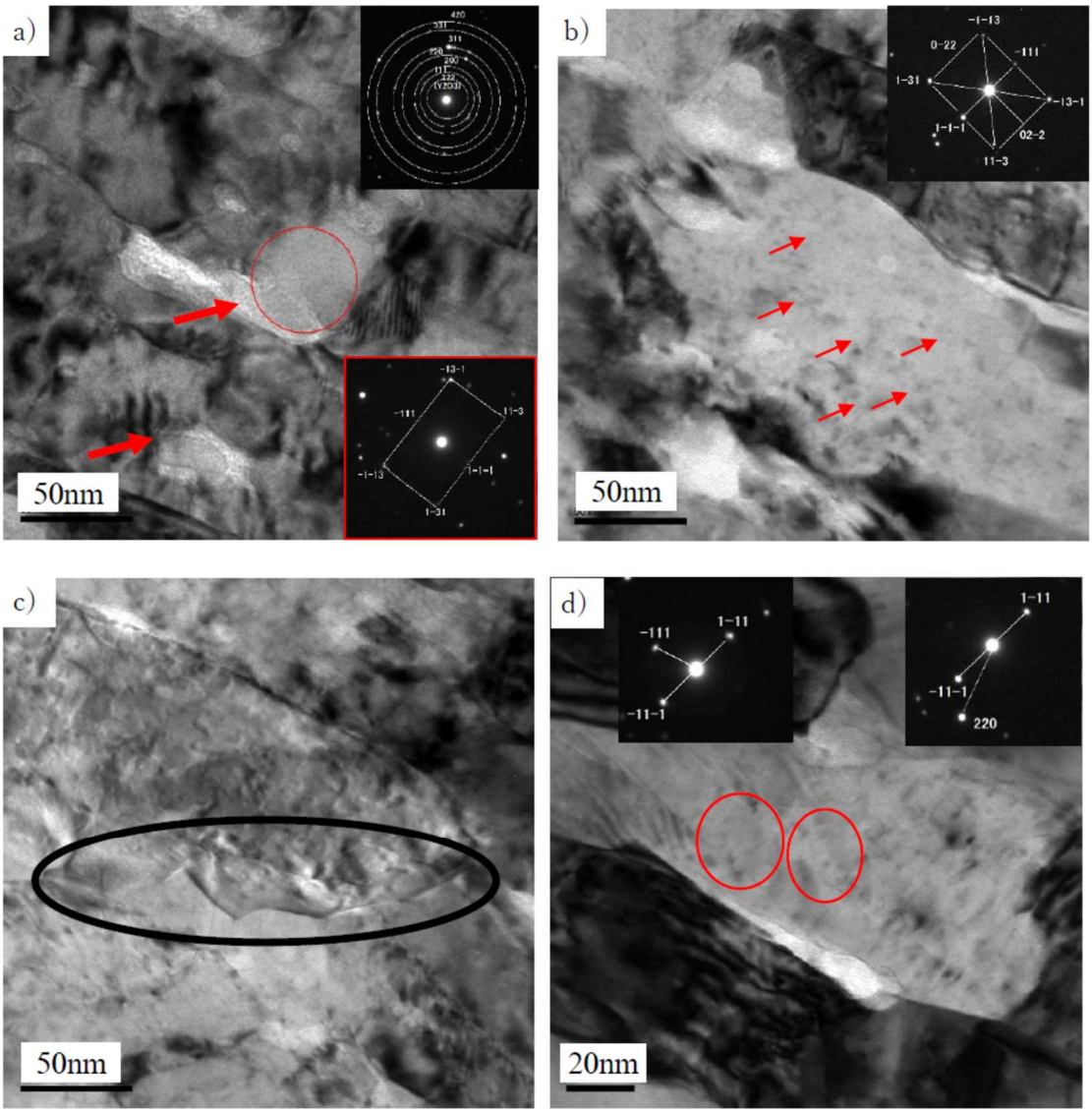

Fig. 10

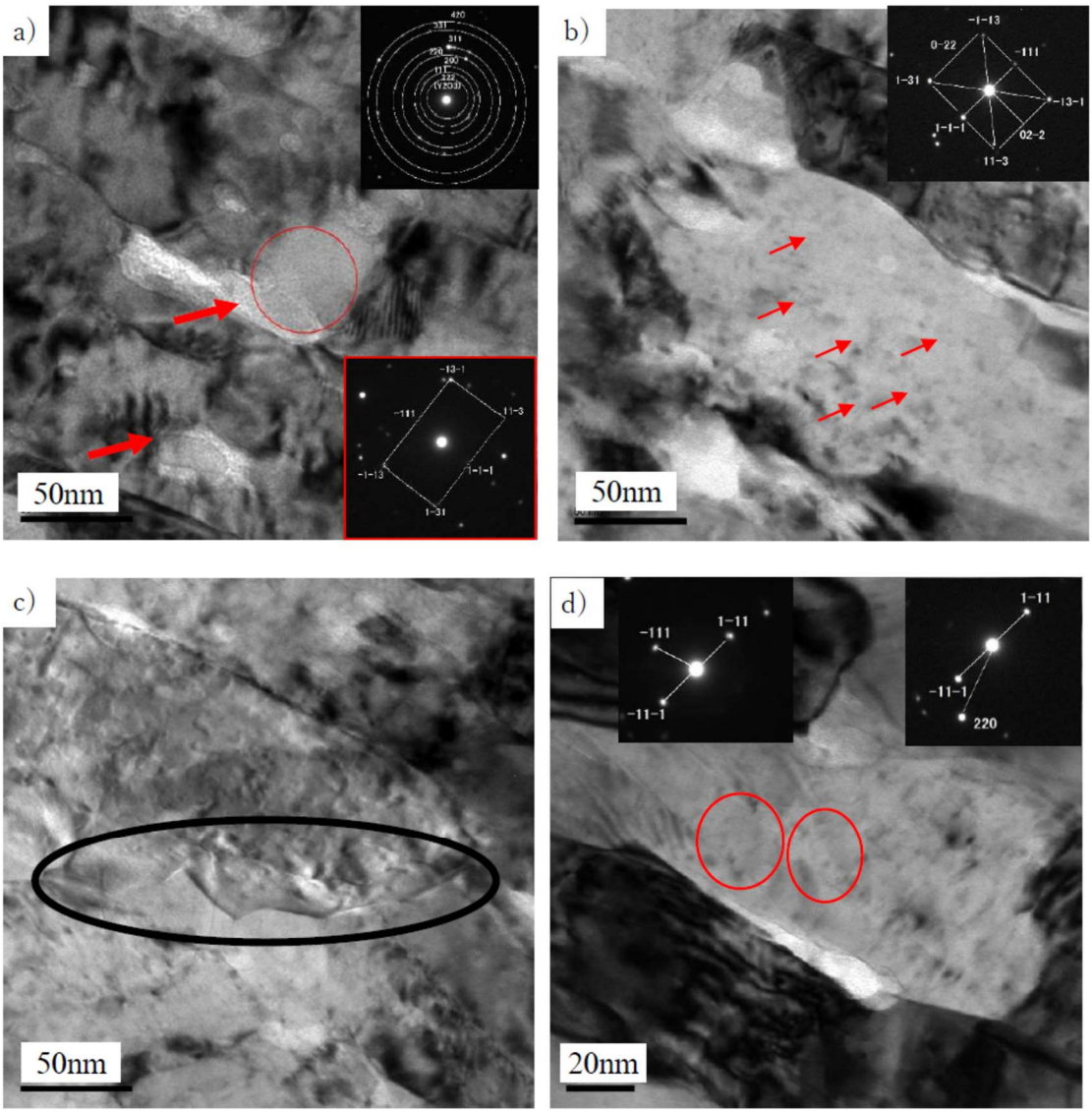

Fig. 10

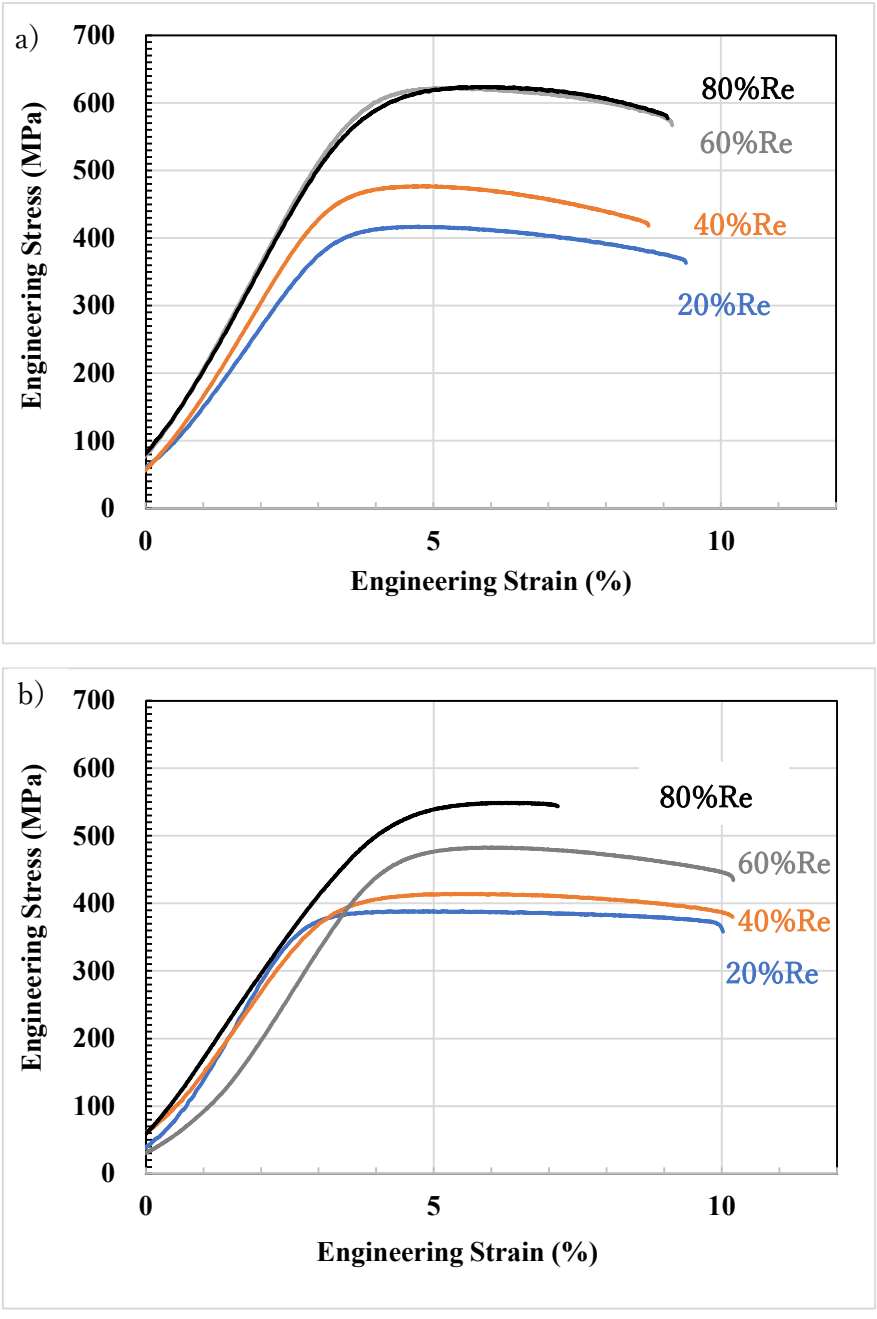
a)
Engineering Stress (MPa)
700
600
500
400
300
200
100
0
0
5
10
Engineering Strain (%)
80%Re
60%Re
40%Re
20%Re
b)
Engineering Stress (MPa)
700
600
500
400
300
200
100
0
0
5
10
Engineering Strain (%)
80%Re
60%Re
40%Re
20%Re

Fig. 11.

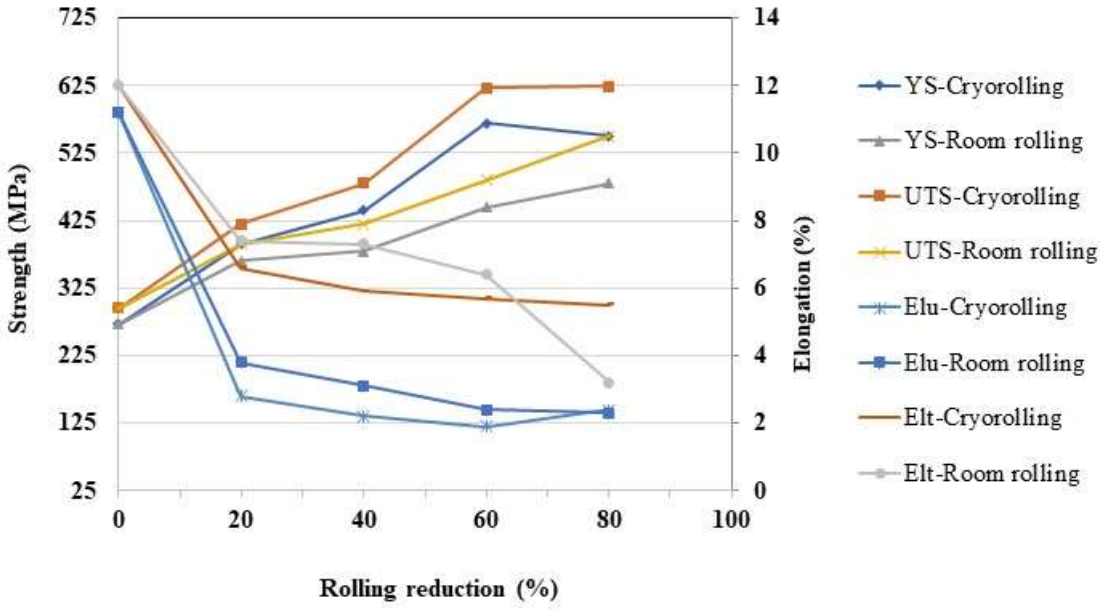
725
625
525
425
325
225
125
25
14
12
10
8
6
4
2
0
0
20
40
60
80
100
Strength (MPa)
Elongation (%)
Rolling reduction (%)
YS-Cryorolling
YS-Room rolling
UTS-Cryorolling
UTS-Room rolling
Elu-Cryorolling
Elu-Room rolling
Elt-Cryorolling
Elt-Room rolling

Fig.12